

Notice: This manuscript has been authored by UT-Battelle, LLC, for the U.S. Department of Energy under contract DE522 AC05-00OR22725. The United States Government retains and the publisher, by accepting the article for publication, acknowledges that the United States Government retains a non-exclusive, paid-up, irrevocable, world-wide license to publish or reproduce the published form of this manuscript, or allow others to do so, for the United States Government purposes. The Department of Energy will provide public access to these results of federally sponsored research in accordance with the DOE Public Access Plan (<https://www.energy.gov/doe-public-access-plan>).

Active Deep Kernel Learning of Molecular Functionalities: Realizing Dynamic Structural Embeddings

Ayana Ghosh*,¹ Maxim Ziatdinov,² Sergei V. Kalinin**^{2,3}

¹Computational Sciences and Engineering Division, Oak Ridge National Laboratory, Oak Ridge, TN, 37831, USA

²Physical Sciences Division, Pacific Northwest National Lab, Richland, WA 99352, USA

³Department of Materials Science and Engineering, University of Knoxville, Knoxville, TN 37996 USA

Abstract:

Exploring molecular spaces is crucial for advancing our understanding of chemical properties and reactions, leading to groundbreaking innovations in materials science, medicine, and energy. This paper explores an approach for active learning in molecular discovery using Deep Kernel Learning (DKL), a novel approach surpassing the limits of classical Variational Autoencoders (VAEs). Employing the QM9 dataset, we contrast DKL with traditional VAEs, which analyze molecular structures based on similarity, revealing limitations due to sparse regularities in latent spaces. DKL, however, offers a more holistic perspective by correlating structure with properties, creating latent spaces that prioritize molecular functionality. This is achieved by recalculating embedding vectors iteratively, aligning with the experimental availability of target properties. The resulting latent spaces are not only better organized but also exhibit unique characteristics such as concentrated maxima representing molecular functionalities and a correlation between predictive uncertainty and error. Additionally, the formation of exclusion regions around certain compounds indicates unexplored areas with potential for groundbreaking functionalities. This study underscores DKL's potential in molecular research, offering new avenues for understanding and discovering molecular functionalities beyond classical VAE limitations.

Email: *ghosha@ornl.gov; **sergei2@utk.edu

1. Introduction

In recent years, the field of molecular discovery¹⁻⁸ has experienced a revolutionary metamorphosis, driven by significant advancements in deep learning (DL) models. These sophisticated algorithms have not only accelerated the pace of molecular research but also discerned the advent of a new era in comprehending and forecasting molecular properties. Within the realm of molecular discovery, DL demonstrates its proficiency in deciphering intricate relationships between molecular structures and properties.⁸⁻¹⁸ This capability empowers researchers to unravel complex mechanisms¹⁹⁻²⁷ and expedite the discovery of novel compounds.

Examples abound in the successful application of DL to molecular discovery, particularly in drug discovery.^{5,6,28-32} Deep learning models play a pivotal role in swiftly identifying potential drug candidates by predicting their efficacy and safety profiles. These models analyze extensive datasets of molecular structures and biological responses, providing valuable insights that streamline the drug development^{23,24,31} process. Moreover, DL models prove invaluable in predicting diverse molecular properties, including toxicity, solubility, and bioactivity. By learning from diverse datasets that encompass molecular structures and experimental outcomes, these models make accurate predictions, significantly economizing time and resources in experimental validation.

The versatility and impact of these models extend across various domains such as quantum chemistry, materials science, prediction of protein structures, and chemical reactions. They moderate the need for computationally expensive quantum mechanical simulations and trial-and-error synthetic chemical routes for efficient exploration of complex molecular interactions, gaining a deeper understanding of dynamic molecular processes. This efficiency is especially beneficial for steering progress in both theoretical chemistry and planning of synthesis.

A typical roster of popular DL models³³⁻³⁸ includes, but *is not restricted to*, graph neural networks (GNNs),³⁹⁻⁴² recurrent neural networks (RNNs),^{22,43-45} convolutional neural networks (CNNs),⁴⁶ autoencoders,^{47,48} Long Short-Term Memory Networks (LSTMs),^{49,50} and attention mechanisms.⁵¹⁻⁵³ GNNs tend to excel in molecular discovery by representing molecules as graphs, with atoms as nodes and chemical bonds as edges. These networks employ message-passing mechanisms to iteratively update node representations based on their local neighborhoods, enabling them to capture intricate relationships between atoms and predict molecular properties. RNNs are well-suited for sequential data, making them valuable for tasks in molecular discovery where molecular structures can be represented as sequences. CNNs prove effective in molecular discovery when applied to molecular images or grids, using convolutional layers to extract spatial features from molecular structures. Autoencoders contribute to molecular representation learning by encoding molecular structures into a lower-dimensional space and then decoding them back to the original space. This process encourages the model to learn meaningful and compact representations of molecules. LSTMs find utility in predicting molecular behavior over time. Attention mechanisms enhance the interpretability of DL models in molecular discovery by assigning varying degrees of importance to different parts of the input, allowing the model to focus on specific features crucial for the task at hand.

While these models are instrumental in unraveling complex relationships within molecular data, active learning strategies⁵⁴ complement them by addressing significant challenges and optimizing the utilization of resources. They boost data efficiency by pinpointing

the most informative instances for labeling, thereby enhancing the efficacy of the learning process, particularly when dealing with limited labeled data. This is especially advantageous in contexts where experimental data collection proves to be both costly and time intensive. Active learning mitigates annotation costs by concentrating on instances that yield the most substantial learning improvements, resulting in noteworthy cost savings, especially in domains such as drug discovery and materials science. Additionally, active learning⁵⁵⁻⁵⁷ adeptly manages imbalanced datasets, navigates diverse regions within the chemical space, and adapts to concept drift over time. By actively selecting demanding instances for annotation, active learning not only contributes to fortifying model robustness but also facilitates transfer learning, amplifying the model's adaptability to related tasks or properties. The iterative characteristic of active learning empowers models to continually enhance their performance, establishing them as invaluable tools for streamlined and effective molecular discovery.

Very importantly, the successes of all the DL models trained as static or within active learning schemes, heavily rely on the molecular embeddings⁵⁸⁻⁶⁰ such as latent variables in VAEs. These in turn are formed as a compression of static descriptors, for e.g., SMILES (Simplified Molecular Input Line Entry System) and SELFIES (Self-referencing Embedded Strings) to effectively represent and connect molecules to different properties. Active learning models leverage these embeddings to select informative instances for labeling, using the condensed representations to measure uncertainty and guide the labeling process toward the most valuable data points, while enhancing data efficiency, reducing annotation costs, and exploring the chemical space effectively.

However, for molecular discovery, it is crucial to leverage molecular embeddings in a manner that establishes connections with the landscape of molecular properties. Therefore, representing molecules in a low-dimensional latent space linked to specific functionalities becomes an integral aspect. These considerations should also be dynamic, encompassing inherent variability, temporal dynamics, and the evolving nature of molecular structures and properties.

Autoencoders are often favored for encoding molecular structures into low-dimensional spaces, owing to their past successes. However, the latent representation generated by autoencoders is not inherently linked to any molecular property; rather, it functions as a compressed, abstract portrayal of the input molecular structure. In the autoencoder context, the model is trained to encode a molecular structure into a lower-dimensional latent space and then decode it back to the original structure, with the latent representation intended to capture essential features in a more concise form.

Although the latent representation may encompass information relevant to molecular properties, the autoencoder⁶¹ itself is not explicitly designed to learn or predict specific properties. The typical training objective for an autoencoder is reconstruction, aiming to minimize the difference between the input and the reconstructed output. Consequently, while the latent representation^{62,63} may capture structural patterns, these patterns may not directly correlate with explicit molecular properties such as atomization energy, molecular enthalpy, dipole moment.

In this study, we showcase the utilization of deep kernel learning (DKL)^{64,65} models with molecular embeddings like SELFIES. This approach allows the direct learning of diverse molecular functionalities in both static and active learning⁶⁶⁻⁶⁸ scenarios. DKL models typically have a hybrid architecture. They consist of both a deep neural network and a kernel function which can be combined within a Gaussian process (GP).⁶⁹⁻⁸⁰ These models employ a hybrid

architecture, incorporating a deep neural network to extract hierarchical features from input data and a kernel function to capture intricate relationships between these features in a higher-dimensional space. The neural network undergoes training through backpropagation, optimizing its parameters, while the kernel function is simultaneously optimized to measure similarity or distance between points in the transformed feature space. DKL finds applications in regression, classification, and dimensionality reduction, excelling in scenarios involving structured data and non-linear relationships. The synergy of deep and kernel approaches enhances generalization and facilitates effective handling of complex, real-world datasets.

2. Mathematical formulations

Below is a brief overview of the DKL principles. For a more comprehensive review, we refer the readers to literature⁸¹. Let's denote input data as X , targets as y , the parameters of NN as Φ with output of the NN as f_{NN} . Typically, the output is obtained through a series of linear transformations followed by non-linear activation functions. The NN transforms the high-dimensional features space (in this case SELFIES) with a feature mapping.

A standard GP can be defined by its mean function $m(\cdot, \cdot)$ and covariance function (kernel) $k(\cdot, \cdot)$. For input X , therefore, the GP is represented as: $f \sim GP(m(X), k(X, X'))$. Here f is a vector of function values at the points in X and $K(X, X')$ is the covariance matrix. In DKL, f_{NN} becomes a part of the kernel while the mean function remains zero.

$$K_{DKL} = K_{RBF}(f_{NN}(X), f_{NN}(X'))$$

The covariance function $K(X, X')$ measures the similarity of distance between points in the transformed feature space. Commonly used kernels include radial basis function (RBF) kernel with hyperparameter l denoting the length scale of the kernel:

$$k(f_{NN}(X), f_{NN}(X')) = \exp\left(-\frac{\|f_{NN}(X) - f_{NN}(X')\|^2}{2l^2}\right)$$

The DKL model parameters (NN weights and RBF kernel length scale) are trained jointly using stochastic variational inference. We then utilize a trained model to derive a posterior predictive distribution for new data points X_* :

$$p(y_* | X_*, X, y) = N(\mu_*, \Sigma_*)$$

μ_*, Σ_* are the posterior mean and covariance, respectively, derived from trained model using standard GP formulas.⁸²

An example implementation of DKL with GP using an open-access Python-based package, namely GPax 0.1.1 (other package dependencies are also listed in the Supporting Information) can be found [here](#).

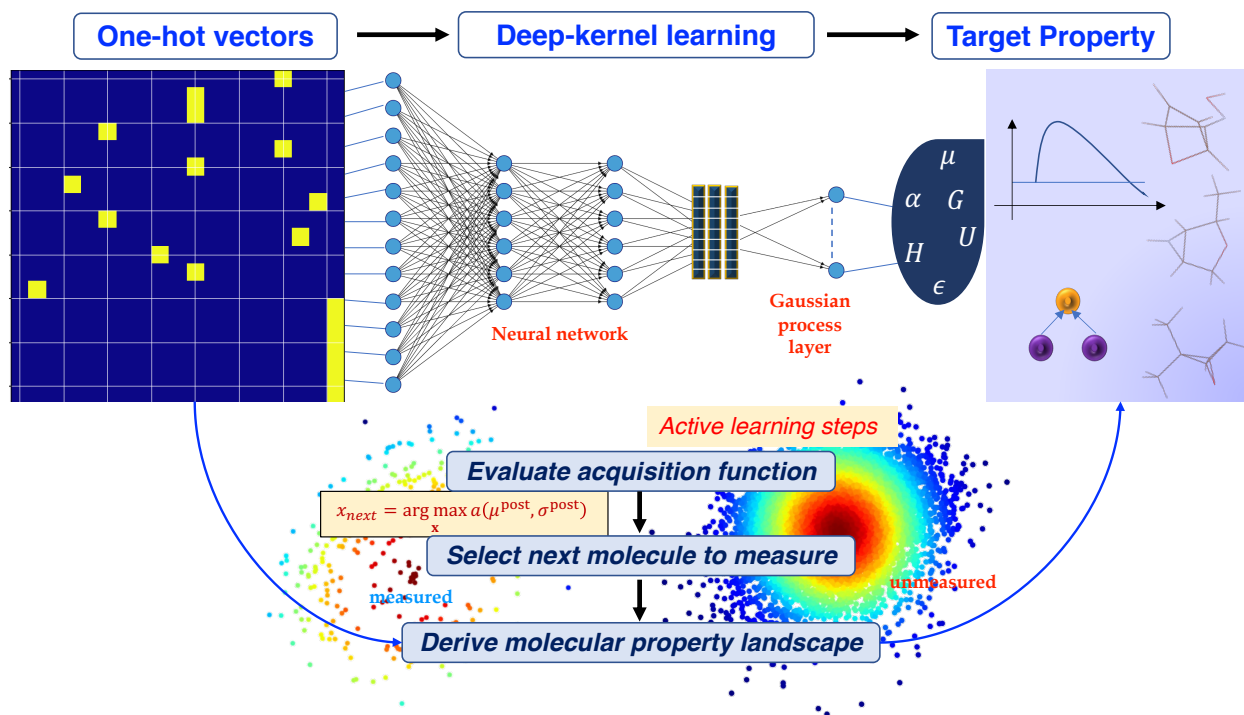


Figure 1: Schematic of active deep kernel learning workflow for deriving molecular property from molecular embeddings.

3. Dataset & workflow

In this study, we have utilized a widely known dataset, QM9 [83], which has served as a benchmark for the development and evaluation of machine learning (ML) models applied to molecular properties prediction. QM9 includes the molecular structures of over 130,000 organic molecules, each represented by its atomic composition and three-dimensional coordinates. The dataset covers a diverse range of chemical compounds, encompassing different functional groups and structural motifs. For each molecule, QM9 provides a set of quantum mechanical properties calculated using density functional theory (DFT) and Hartree-Fock methods. These properties include total energy, enthalpy, free energy, electronic spatial extent, zero-point vibrational energy, and more.

For each molecule, we have computed the one hot vectors within SELFIES embedding with a goal to directly predict functionalities such as enthalpy, dipole moment from the embeddings. In addition, we also calculate molecular features such as molecular weight (MW), topological polar surface area (TPSA), molar log P (molelogP), hydrogen bond donor (HBD) and acceptor (HBA) using the python implementation of RdKit package. The DKL models are trained on 5,000 molecules randomly chosen from the entire QM9 dataset to explore embeddings. As an illustration, we utilize these few features as intermediate targets to train DKL to illustrate how the DKL latent space connects to such features as well as other molecular properties. Next, we run the DKL as an active learning process - meaning that all the features are available (or equivalently our search space is defined), whereas targets are becoming available sequentially, as would be the case for (expensive) experiments. Here, we define our

hyperparameters namely, the number of initial samples (for active learning), number of exploration steps, batch size for active learning, and batch size for reconstructions. Here, we consider our example target as enthalpy with ~1% of the 5,000 molecules to initiate the active learning process to reconstruct the functionality over the entire chemical space. Figure 1 shows a schematic of the workflow of the active DKL as considered in the study. The workflow has been replicated for a randomly selected set of 12,000 molecules, accompanied by a systematic examination of the resources required to address the scalability aspects of the workflow.

In the workflow, our initial step involves (a) training DKL models using the hot-vectors for selected molecular features with potential dependencies on DFT-computed targets. Subsequently, (b) the active learning phase commences with a DFT-computed target. (c) We monitor the mean and standard deviations of the next points of measurement as predicted by the DKL model, iteratively trained in each cycle, along with the complete DKL model established in step (a). This detailed tracking provides comprehensive insights into the trajectories of the active learning process, revealing how the chemical space is traversed during the exploration-exploitation steps. It is important to note that, for up to 12k molecules, we employ the exact GP to train the DKL models, ensuring precise computation of covariance matrices. As a result, the uncertainty measurements pertaining to the trajectories exhibit a high level of accuracy, directly influencing molecular discovery. Example implementations of the VAE and DKL models are provided with accompanying notebooks via the [Github repository](#).

4. Results & Discussion

Target properties: Dipole moment, Enthalpy, and Gibb's Free Energy

We have utilized 5,000 and then 12,000 molecules randomly selected from the comprehensive QM9 dataset for our computations. Specifically, we choose dipole moment, enthalpy and Gibb's free energy as the target molecular properties and created three randomized subsets of the same dataset size to implement the DKL workflow. The QM9 dataset includes various target properties such as HOMO-LUMO gap, atomization energy, and enthalpy of formation. Investigating dipole moment is crucial as it provides valuable insights into the spatial distribution of electric charge within a molecule. This understanding is fundamental for elucidating polarity and predicting intermolecular interactions.

For molecules, it relates to polarity which in turn, influences properties such as solubility and chemical reactivity. For systems such as polymers, dipole moment also determines their electrical properties and behavior in electronic devices. Mathematically, the dipole moment is calculated as the product of the charge and the displacement vector. Analyzing dipole moments aids in predicting molecular behavior and designing materials with specific electrical characteristics. As shown in Figure 2, most of the molecules in all three subsets exhibit negligible dipole moments, suggesting a symmetric distribution of charges or cancellation of dipole moments within the structures. This characteristic might influence the compounds' behavior in solvents or interactions with other molecules, as lower dipole moments generally imply reduced polarity and weaker interactions with polar environments. We note that molecular features such as molar LogP, TPSA, MW, HBD, HBA, valence electrons, partial charges, rotatable bonds, ring counts, and stereocenters, may also collectively contribute to the dipole moments of molecules. LogP and TPSA provide insights into lipophilicity and polar interactions,

influencing the overall polarity of molecules. MW, valence electrons, and partial charges impact the electronic structure and response to external electric fields, affecting dipole moments. HBAs and HBAs influence polar interactions, contributing to dipole formation. The number of rotatable bonds affects conformational flexibility, potentially influencing dynamic charge distributions. Additionally, the presence of cyclic structures (ring counts) and chiral centers (stereocenters) can impact the three-dimensional arrangement of atoms, contributing to variations in dipole moments. Understanding these properties collectively enhances our comprehension of how molecules interact with their environment and exhibit diverse dipole characteristics.

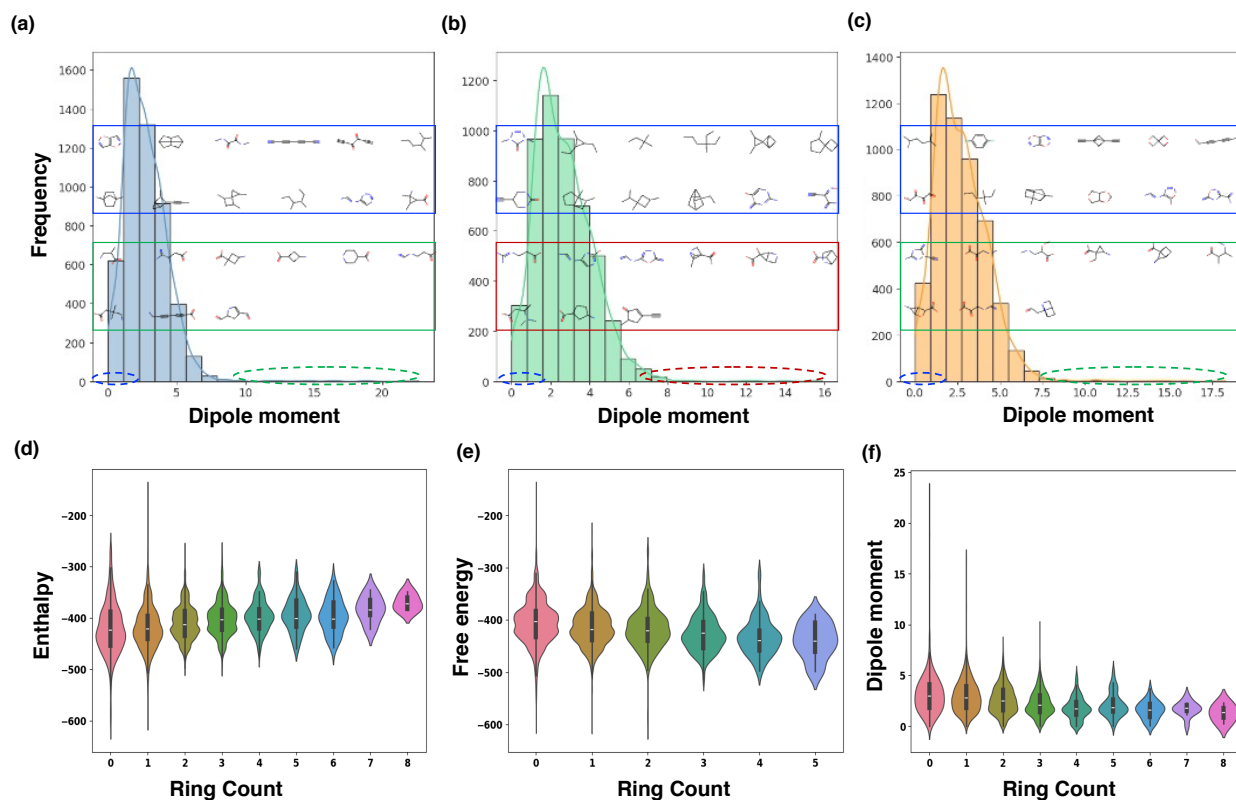


Figure 2: The dipole moment distribution of molecules is illustrated for three (a-c) randomly sampled datasets of size 5,000. Selected molecules from the tails of the distributions are overlaid on the histograms. Distributions of selected properties (e.g., enthalpy (d), Gibb’s free energy (e) and dipole moment (f)) as listed in QM9 with respect to molecular features (e.g., ring counts, rotatable bond counts).

While predominantly featuring weak dipole moments in all the subsets, certain molecules in the first subset (Figure 2a) display notably high dipole moments, indicating enhanced polarity and a propensity for robust interactions with electric fields or polar surroundings. For example, the molecule represented by the SMILES string NC=[NH+]C1=CN=N[N-]1 (~13.73 D) exhibits a substantial dipole moment, primarily attributed to the presence of charged nitrogen atoms. Likewise, CC1C(C([O-])=O)C1(C)[NH3+] has a considerable dipole moment (~14.62 D), likely influenced by the charged nitrogen and oxygen atoms within its structure. Additionally, compounds like [NH3+]C1CC(C1)C([O-])=O and [O-]C(=O)CCNC=[NH2+] showcase elevated

dipole moments (~16.54 D and 18.69 D), suggesting the active participation of charged functional groups. These molecules characterized by heightened dipole moments demonstrate a combination of charge separation, polar bonds, and the presence of charged species, underscoring their potential reactivity and responsiveness to electrostatic interactions. Similarly in the second subset (Figure 2b) N=C1[N-]N=C(NC=[NH2+])O1, for example, features a high dipole moment (~11.89 D) attributed to the presence of charged nitrogen and oxygen atoms. Similarly, compounds like CC1[NH+]2CC1(C2)C([O-])=O and OC1(C2C[NH2+]C12)C([O-])=O showcase high dipole moments (~12.22 D, 12.61 D), likely influenced by charged nitrogen, oxygen, and carbon atoms within their structures. In subset 3 (Figure 2c), there are molecules such as C[NH2+]CC(=O)C([O-])=O and C[NH2+]CC(OC)C([O-])=O exhibit high dipole moments (~12.92 D, 13.82 D), indicating influence of charged functional groups and the presence of polar bonds.

Additionally, consideration of Gibbs free energy (Figure 2(d)), enthalpy (Figure 2(e)), and rotatable bonds (rotb) (Figure 2(f)) provides insights into the thermodynamic and structural aspects of these molecules, enriching our understanding of their reactivity and behavior in various environments. Computational determination of enthalpy and Gibbs free energy for molecules is intricate and computationally demanding. Methods like DFT and coupled cluster, while providing accurate results, require substantial computational resources, especially for complex molecules. Optimization of molecular geometry and calculation of thermodynamic properties involve solving intricate equations, contributing to computational expense. Consideration of temperature and pressure adds further complexity. This has provided us with further motivations to apply the DKL algorithm to predict these molecular properties as additional targets.

VAE latent spaces

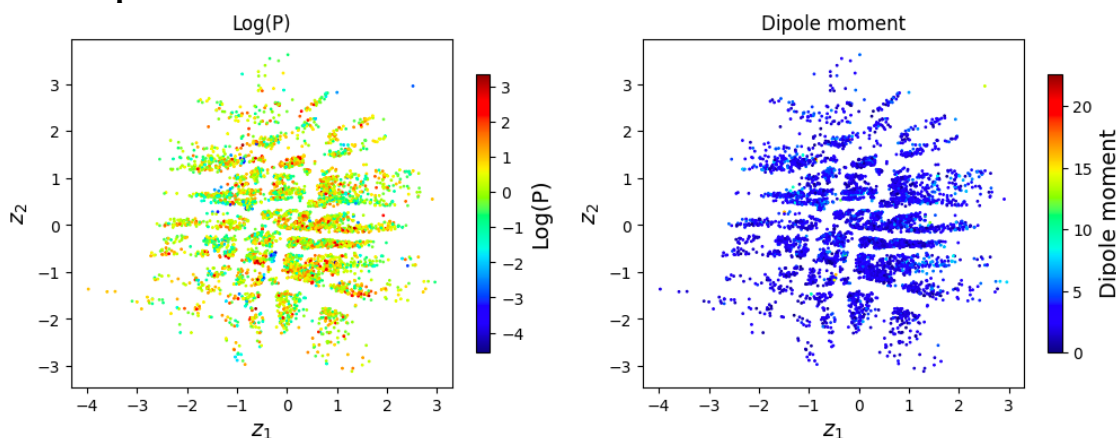


Figure 3: Latent space as obtained from VAE model (5,000 molecules) trained using one-hot vectors.

Our discussion begins with an exploration of conventional VAEs, which are among the widely used approaches for learning from high-dimensional molecular datasets. This initial focus serves to emphasize on the potential limitations that analyzing latent space distributions may not yield extensive information about the target properties. We have trained a traditional VAE as implemented in the [pyroVED](#) implementation using the one-hot vectors as inputs for 5k

molecules. The corresponding latent space distributions are shown in Figure 3. As briefly mentioned earlier, the main principle of VAE relies on mapping the input data to a low dimensional latent space via the encoder part and the decoder part reconstruct the input data from the latent space. In contrast to the DKL models, here the latent space is obtained without direct consideration of the target properties as shown in Figure 3. It is evident that not much information can be extracted from such latent distributions. Within these models, there is no direct optimization based on targets and therefore not much information about the molecular property landscapes can be obtained as compared to DKL models. An accompanying notebook can be found with example VAE implementations within the [Github repository](#).

DKL latent spaces for target properties

Standard DKL models

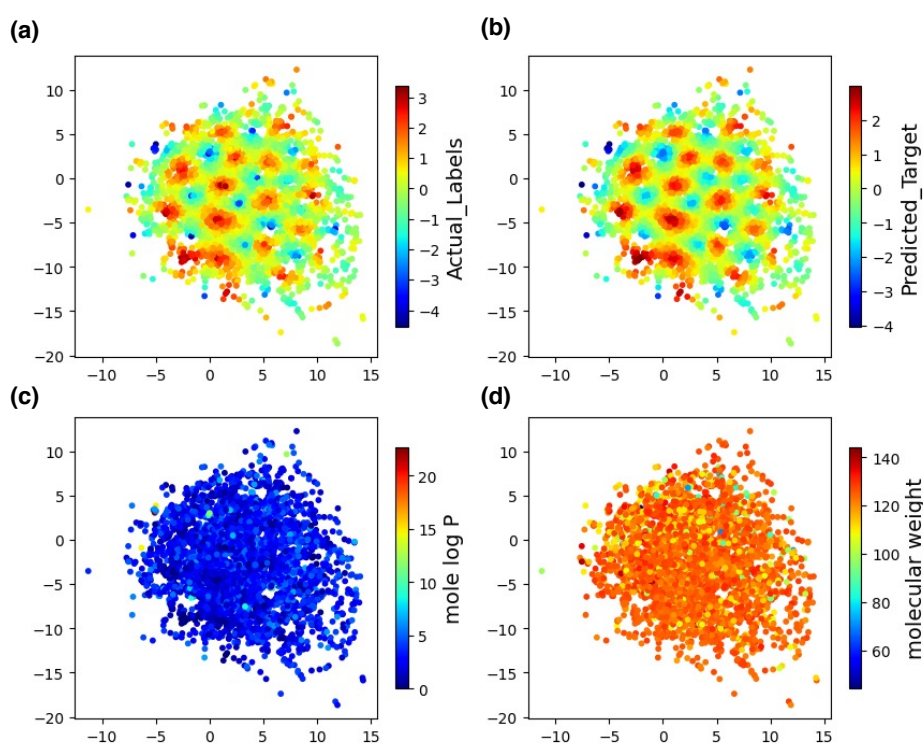


Figure 4: Latent space as obtained from DKL model (5,000 molecules) trained for target property molar log P using one-hot vectors.

Unlike the VAE models, the latent space (Figure 4 and 5) generated by the DKL models connects to the molecular properties. It then becomes possible to investigate selected neighborhoods of molecules with respect to specific targets. Figure 6 is an example visual representation of the selected molecules with closest Euclidean distances to molecule represented with SMILE string CC12CCC(C)(CC1)C2 with the highest molelogP value of ~ 2.767 . This down-selection process suggests a correlation between Euclidean distances and predicted molelogP. The molecules in the closest neighborhood, i.e., those with shorter Euclidean distances, may be considered more structurally similar. Generally, such a high value of molelogP indicated that the molecule maybe somewhat lipophilic which may affect phramokinteic

properties. Compounds with favorable lipophilicity characteristics, can be crucial in drug discovery and other applications. Based on the SMILE representations of the molecules in the closest neighborhood, there are a few structural similarities that are evident. All the systems include cycloalkane or cycloalkene structures with varying substituents. They exhibit similar arrangements of carbon atoms in cyclic or bridged cyclic forms, suggesting a degree of structural resemblance with the reference structure.

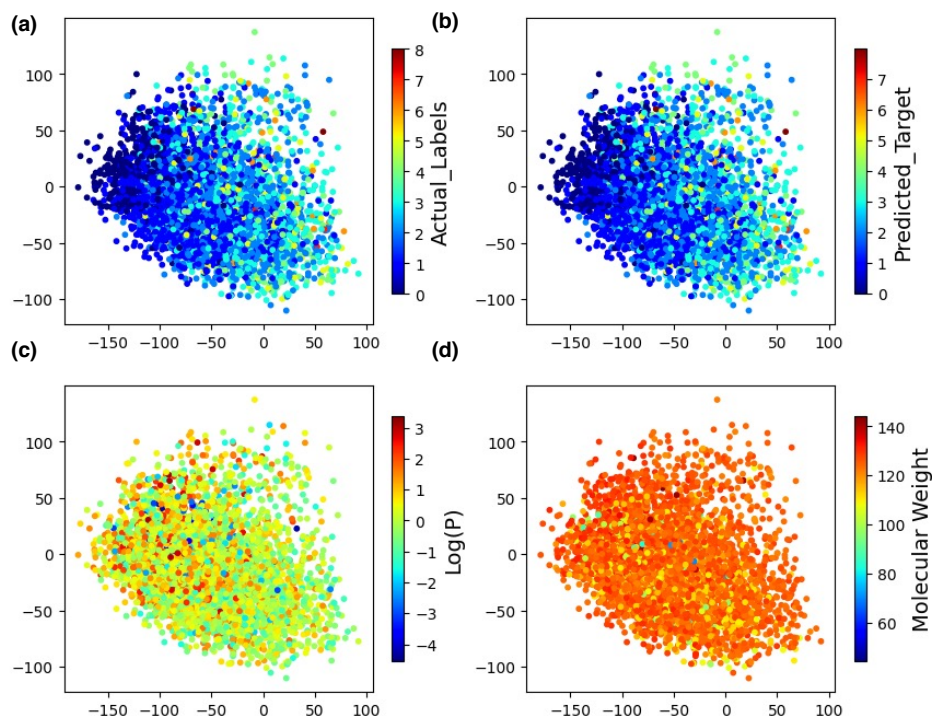


Figure 5: Latent space as obtained from DKL model (5,000 molecules) trained for target property, number of rings using one-hot vectors.

We have conducted similar studies for other targets such as ringct and rotb, respectively. For ringct, the down selection leads to curation of molecules with SMILES representations, N#CCC1CCCO1, CC(CC#N)N(C)C, CNC1(COC1)C(C)=O, OC1CC(NC1=N)C#N, CC1C2CC1(C)C1CN21, OC1CC=C2COCC1, CC1CC1(C)CCC#C, CCC1=COC=C1C, COCC1=C(N)C=CO1. They all contain a mixture of functional groups, including nitrogen-containing rings, carbon-carbon double bonds, and cyano groups.

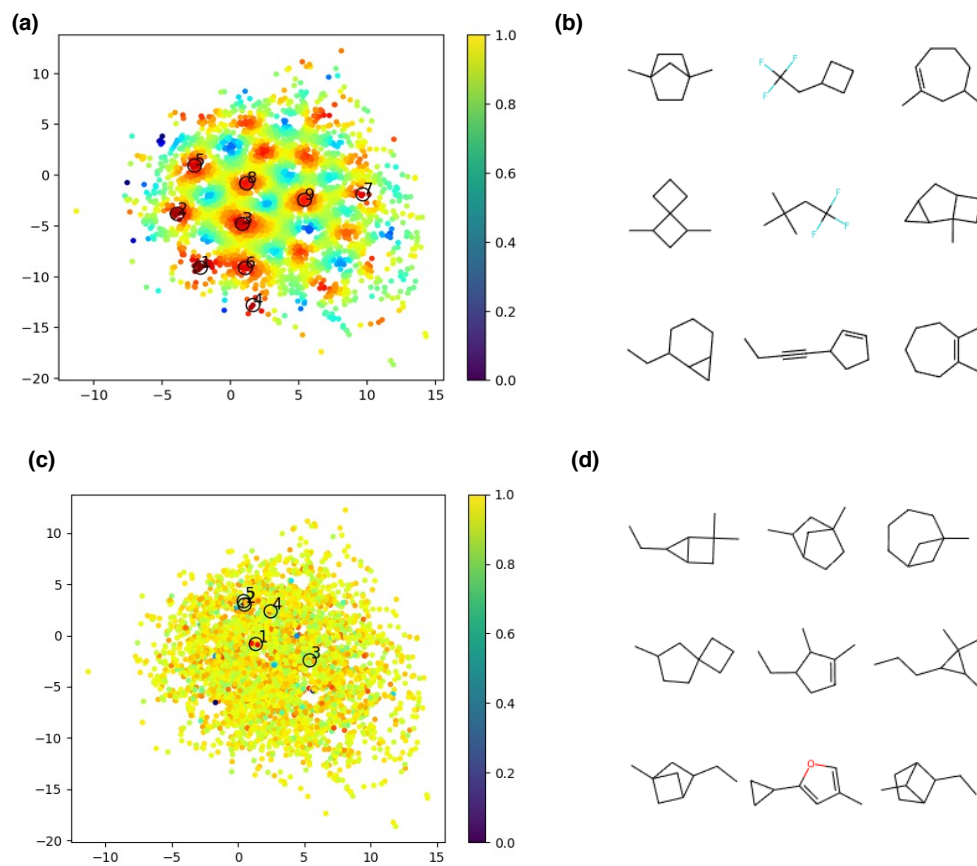


Figure 6: Selected molecules with highest molar log P values as predicted by the DKL models, and identified molecules located at the closest vicinity of these selected molecules within (a, c) the latent space and (b, d) using molecular diagrams, respectively.

In general, presence of ring like substructures results in increase in molecular complexity, rigidity toward forming conformations, synthesis along with affecting other properties such as its solubility, lipophilicity, and stability. Based on the highest rotb of 6, we have utilized OCCCOCCO as reference structure to locate the nearest neighbors. The neighborhood comprises molecules such as CCC(CCO)OC=O, OCCOCC(O)C=O, CCC(C)OCCC=O, NCC[NH2+][O-]C=O, CCC(CCOC)C=O, OCC(CO)OCC=O, COCCOCC(C)C, CCCCCCC(C)O, CCCCCOC=NC. They all collectively exhibit a substantial number of rotatable bonds that indicate a certain degree of flexibility to form conformations. They all include multiple aliphatic chains and oxygen-containing functional groups. The presence of oxygen atoms and carbonyl groups suggests potential similarities in their chemical reactivity and interactions.

Active DKL models

In the next step of the workflow, we perform the active DKL routine for the same set of 5,000 and 12,000 molecules to predict an assortment of DFT-computed targets such as dipole moment, enthalpy and Gibbs free energy as listed in QM9 dataset. The active learning loop is initiated by selecting <2% of the data (100 molecules) from these subsets. Within each iteration,

the DKL is trained with the unmeasured points, followed by computation of acquisition function (summation of mean and standard deviation). The optimized point suggested by maximizing (or minimizing) this objective function becomes the next point of measurement. Additionally, we also retrieve mean and standard deviations of the next point of measurements from one of the standard DKL models trained before within the first step. This is to compare any existing correlations ingrained in the predictions by the standard DKL models endpoints (e.g., molelogP, ringct and rotb) with those by the active DKL models endpoints (e.g., dipole moment, enthalpy, and Gibb's free energy). The active learning loop is repeated until all points in the subsets have been evaluated.

Figure 7 shows the latent space distributions of the measured, unmeasured points with corresponding ground truths as well as prediction uncertainties for predicting enthalpy. The Supporting Information also includes the distributions for the other two target properties. Here, the error is evaluated by taking the difference between predicted from the ground truth (as listed in QM9) and uncertainty representations the respective standard deviations.

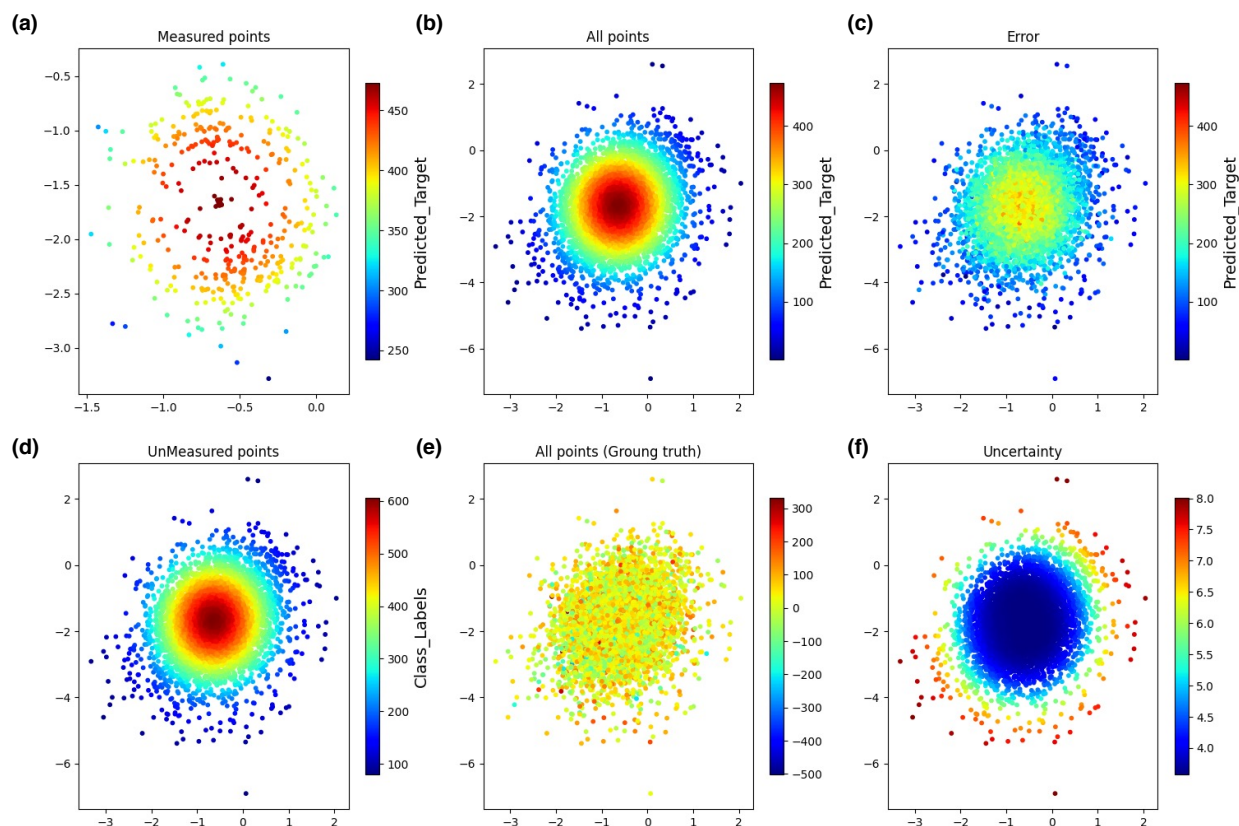


Figure 7: Latent space distributions of (a) measured points, (b) corresponding predictions (c) error (predicted - computed), (d) unmeasured points, (e) ground truth and (f) associated prediction uncertainty to predict enthalpy of molecules using active DKL model.

There are distinct regions in the latent spaces indicating similar behavior as observed for the standard DKL models. The accuracy is much less for all the targets as evident from the uncertainty maps. This is somewhat expected since the active DKL models were trained using a

notably small number of molecules, which may not adequately capture the diverse range of molecular structures present in the entire subsets.

Lower values of enthalpy and Gibb's free energy typically indicate greater thermodynamic stability of molecules. More specifically, systems with low enthalpy values suggest energetically favorable states within which atoms are already arranged in configurational states with low energy levels whereas low free energy corresponds to greater tendency for the system to move towards a stable equilibrium. On the other hand, most of the molecules within the entire subset exhibit weak polarity, characterized by low dipole moments. This contributes to the challenges in accurately predicting the properties of those with higher dipole moments. The less precise predictions for the latter group arise from the models struggling to effectively capture the embeddings associated with stronger polarity, which is less commonly represented in the overall dataset.

To gain deeper insights into the discovery of molecules within the chemical space during active learning and explore potential correlations, we can examine how the suggestions (measurement points) made by active DKL models align with those provided by the standard DKL models trained originally for a set of different targets. For instance, we can investigate whether the mean and standard deviations of the predictions of a standard DKL model trained for molelogP exhibit correlations with recommendations provided by an active DKL model trained for dipole moment. There are very weak linear correlations as indicated by small Pearson correlation coefficients (<0.1) between the respective mean and standard deviations from each of the models for all three (molelogP-dipole moment), (ringct-enthalpy) and (rotb-free energy) pairs. This does not necessarily mean that complex molecular interactions might be at play which may not be straightforwardly linear in nature. To further understand this, we have performed a post-processing analysis to compute Tanimoto similarities between 20 selected molecules picked from the sets of measured and unmeasured points as shown in Figure 8. The Tanimoto similarity provides a quantitative measure of how similar two sets are based on the presence or absence of specific features. For example, the molecules CC1NC(=O)C1(N)C#C (dipole moment ~ 3.068 D, molelogP ~ -1.164) and C1C2CNC3=C2N1C=C3 (dipole moment ~ 1.650 D, molelogP ~ 1.011) display a notably high similarity, indicating potential structural resemblance. In addition, molecule with high dipole moment with low molelogP is more likely to be more water soluble, which could be important for drug discovery and related applications. Both have cyclic structures with nitrogen atoms. While the presence of carbonyl group in the first molecule carries signature of potential for hydrogen bonding and interactions involving the oxygen atom of the carbonyl group, the latter may participate in various bonding interactions, and the aromatic ring structure suggests the possibility of π - π stacking interactions.

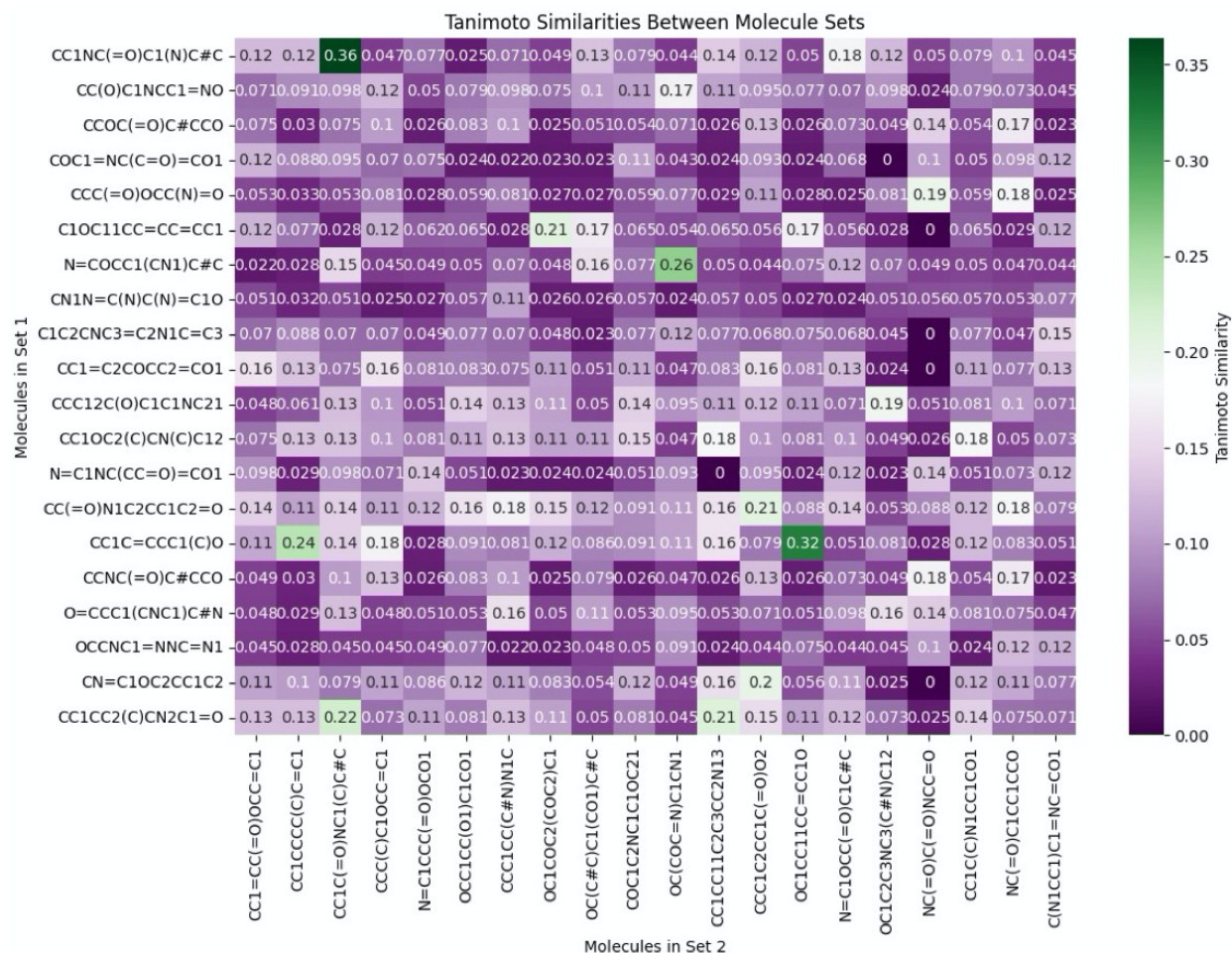


Figure 8: Heatmap representing the Tanimoto similarity indices between 20 molecules selected from the unmeasured and measured points as found during the active DKL training for dipole moment.

We have also included the active learning trajectory means with standard deviations as error bars for active DKL models for targets such as dipole moment, enthalpy, and free energy, respectively in the Supporting Information. The predictions are made in batches of 250 points. This analysis aims to uncover patterns and relationships between different molecular properties, shedding light on how the active learning process influences the exploration of the chemical space and whether certain molecular features are interrelated. Understanding these correlations can enhance our comprehension of the chemical landscape and inform more targeted and effective strategies for molecular discovery. We note that for other datasets with randomly selected molecules, the latent space distributions may vary although the uncertainties in predictions remain within the confidence bound as obtained here.

Scalability aspect

The validity of all observations remains consistent for DKL models trained with 12,000 molecules, irrespective of whether they were trained using the complete subsets or within the active learning workflow. We have included these results separately in the Supporting

information. We would like to point out that training DKL model with 12,000 data points require substantial use of computational resources. On a single GPU node with 32GB memory, it may take up to an hour to train a standard DKL model. However, the challenge lies in computing the uncertainty estimates using the exact GP which requires a ton of memory allocation. We have performed a systematic study to showcase the computational resources and the results are included in the Supporting Information.

Tasks such as molecular discovery with targeted properties may require very accurate estimations of the associated prediction uncertainties. But we also note that within the active learning workflow, the next point of measurement is guided by estimation of relative uncertainties. Hence, in this case, it may be possible to utilize other approximation for uncertainty measurements to decrease the need for such high memory allocations. Some common approximations involve sparse methods to handle computational scalability. Consequently, the researcher might have to decide between an accuracy-to-computationally feasibility trade-offs to drive the task of molecular design and discovery.

5. Conclusions

In summary, we have implemented an active Deep Kernel Learning (DKL) workflow to gain insights into diverse molecular functionalities. This encompasses features ranging from those readily estimable directly from canonical SMILES string representations to properties requiring computationally expensive first-principles calculations. An essential aspect is the utilization of DKL models, which employ Gaussian process models to establish connections with the target variables. The training of the DKL models has allowed us to derive latent spaces with more distinctive patterns connected to endpoints as compared to those obtained through variational autoencoders or other commonly employed models in the literature.

While molecular features computed from SMILES strings provide initial insights into molecules, relying solely on them may not suffice for accurate predictions of other molecular properties such as enthalpy, free energy, or dipole moment. The one-hot vector representations and the corresponding embeddings created by DKL models prove to be more robust for extracting relationships between molecular structure and properties. Our analyses further demonstrate the potential to derive design principles for targeted properties by uncovering underlying correlations in the data. The dynamically learned molecular embeddings within the active learning framework are designed to address real-time molecular design and the exploration of undiscovered chemical spaces. This has the potential to yield benefits for both the physical sciences and machine learning communities.

6. Acknowledgements

This research (A.G.) is sponsored by the INTERSECT Initiative as part of the Laboratory Directed Research and Development Program of Oak Ridge National Laboratory, managed by UT-Battelle, LLC, for the U.S. Department of Energy under contract DE-AC05-00OR22725. This work (S.V.K.) (workflow prototyping) was supported by the US Department of Energy, Office of Science, Office of Basic Energy Sciences, as part of the Energy Frontier Research Centers program: CSSAS—The Center for the Science of Synthesis Across Scales—under Award No.DE-SC0019288, located at University of Washington, DC.

7. Author Contributions

A.G. implemented the DKL active learning workflow for QM9 dataset and wrote the manuscript draft. S.V.K. implemented the prototype workflow. M.Z. developed the original DKL active learning as implemented in GPax package. All co-authors have participated in manuscript writing and discussion.

8. Code Availability

The variational autoencoder, deep kernel learning, active learning workflow illustrative codes can be freely accessed via [Github repository](#).

9. Data Availability

The datasets used in this work are freely accessible via [Github repository](#).

10. Conflicts of Interest

The authors declare no competing interests.

References

- 1 Alexander Tropsha, J. g. Computational methods for drug discovery and design. *Journal of medicinal chemistry* **59.1**, 1 (2016).
- 2 Bartók, A. P. e. a. Machine learning unifies the modeling of materials and molecules. *Sci. Adv.* **3** (2017).
- 3 Barzilay, W. P. W. a. R. Applications of Deep Learning in Molecule Generation and Molecular Property Prediction. *Accounts of chemical research* **54**, 263-270 (2021).
- 4 J. Phillip Kennedy, L. W., Thomas M. Bridges, R. Nathan Daniels, David Weaver, and Craig W. Lindsley. Application of Combinatorial Chemistry Science on Modern Drug Discovery. *Journal of Combinatorial Chemistry* **10**, 345-354 (2008).
- 5 Jun Xu, A. H. Cheminformatics and drug discovery. *Molecules* **7**, 566-600 (2002).
- 6 Lo, Y. C., Rensi, S.E., Torng, W. and Altman, R.B. Machine learning in chemoinformatics and drug discovery. *Drug Discovery Today* **23**, 1538-1546 (2018).
- 7 Tkatchenko, A. Machine learning for chemical discovery. *Nature Communications* **11** (2020).
- 8 Butler, K. T., Davies, D. W., Cartwright, H., Isayev, O. & Walsh, A. Machine learning for molecular and materials science. *Nature* **559** (2018).
- 9 Noé, F., Tkatchenko, A., Müller, K.-R. & Clementi, C. Machine learning for molecular simulation. *Ann. Rev. Phys. Chem.* **71** (2020).
- 10 Takahashi, S., Masamichi Takahashi, Shota Tanaka, Shunsaku Takayanagi, Hirokazu Takami, Erika Yamazawa, Shohei Nambu et al. A new era of neuro-oncology research pioneered by multi-omics analysis and machine learning. *Biomolecules* **11** (2021).
- 11 Toyao, T., Zen Maeno, Satoru Takakusagi, Takashi Kamachi, Ichigaku Takigawa, and Ken-ichi Shimizu. Machine learning for catalysis informatics: recent applications and prospects. *ACS Catalysis* **10**, 2260-2297 (2019).
- 12 Wenhong Yang, T. T. F., and Wen-Hua Sun. Machine Learning in Catalysis, From Proposal to Practicing. *ACS Omega* **5**, 83-88 (2020).
- 13 Sun, W., Yujie Zheng, Ke Yang, Qi Zhang, Akeel A. Shah, Zhou Wu, Yuyang Sun et al. Machine learning–assisted molecular design and efficiency prediction for high-performance organic photovoltaic materials. *Science Advances* **5**, eaay4275 (2019).
- 14 B. Cao, L. A. A., A. O. Oliylyk, E. J. Luber, B. C. Olsen, A. Mar, J. M. Buriak. How to optimize materials and devices via design of experiments and machine learning: Demonstration using organic photovoltaics. *ACS nano* **12**, 7434-7444 (2018).
- 15 J. Hachmann, R. O.-A., S. Atahan-Evrenk, C. Amador-Bedolla, R. S. Sánchez-Carrera, A. Gold-Parker, L. Vogt, A. M. Brockway, A. Aspuru-Guzik,. The Harvard clean energy project: Large-scale computational screening and design of organic photovoltaics on the world community grid. *J. Phys. Chem. Lett.* **2**, 2241-2251 (2011).
- 16 K. Sun, Z. X., S. Lu, W. Zajaczkowski, W. Pisula, E. Hanssen, J. M. White, R. M. Williamson, J. Subbiah, J. Ouyang, A. B. Holmes, W. W. H. Wong, D. J. Jones. A molecular nematic liquid crystalline material for high-performance organic photovoltaics. *Nat. Commun.* **6** (2015).

- 17 Gómez-Bombarelli, R. e. a. Design of efficient molecular organic light- emitting diodes by a high-throughput virtual screening and experimental approach. *Nature Materials* **15** (2016).
- 18 Er, S., Suh, C., Marshak, M. P. & Aspuru-Guzik, A. Computational design of molecules for an all-quinone redox flow battery. *Chem. Sci.* **6**, 885 (2015).
- 19 Segler, M. H. S., Preuss, M. & Waller, M. P. Planning chemical syntheses with deep neural networks and symbolic AI. *Nature* **555** (2018).
- 20 Fedorov, D. V., Sadhukhan, M., Stöhr, M. & Tkatchenko A. Quantum- mechanical relation between atomic dipole polarizability and the van der Waals radius. . *Physical Review Letters* **121** (2018).
- 21 Wilkins, D. M. e. a. Accurate molecular polarizabilities with coupled cluster theory and machine learning. *Proc. Natl Acad. Sci.* **116** (2019).
- 22 Zhenpeng Zhou, X. L., and Richard N. Zare. Optimizing Chemical Reactions with Deep Reinforcement Learning. *ACS Cent. Sci.* **3**, 1337-1344 (2017).
- 23 Christos Xiouras*, F. C., Gustavo Lunardon Quilló, Mihail E. Kavousanakis, Dionisios G. Vlachos, and Georgios D. Stefanidis. Applications of Artificial Intelligence and Machine Learning Algorithms to Crystallization. *Chem. Rev.* **122** (2022).
- 24 Ayana Ghosh, L. L., Kapildev K Arora, Bruno C Hancock, Joseph F Krzyzaniak, Paul Meenan, Serge Nakhmanson, Geoffrey PF Wood. Assessment of machine learning approaches for predicting the crystallization propensity of active pharmaceutical ingredients. *CrystEngComm* **8**, 1215-1223 (2019).
- 25 Shen, C., Junjie Ding, Zhe Wang, Dongsheng Cao, Xiaoqin Ding, and Tingjun Hou. Shen, Chao, et al. "From machine learning to deep learning: Advances in scoring functions for protein–ligand docking. *Computational Molecular Science* **10** (2020).
- 26 Coley, C. W., William H. Green, and Klavs F. Jensen. Machine learning in computer-aided synthesis planning. *Accounts of chemical research* **51**, 1281-1289 (2018).
- 27 Gromski, P. S., Jarosław M. Granda, and Leroy Cronin. Universal chemical synthesis and discovery with ‘The Chemputer’. *Trends in Chemistry* **2**, 4-12 (2020).
- 28 José Jiménez-Luna , F. G. a. G. S. Drug discovery with explainable artificial intelligence. *Nature Machine Intelligence* **2**, 573-584 (2020).
- 29 al., B. N. e. Large scale comparison of QSAR and conformal prediction methods and their applications in drug discovery. *J. Cheminf.* **11** (2019).
- 30 Vamathevan, J., Dominic Clark, Paul Czodrowski, Ian Dunham, Edgardo Ferran, George Lee, Bin Li et al. Applications of machine learning in drug discovery and development. *Nature Reviews drug discovery* **18**, 463-477 (2019).
- 31 Ekins, S., Ana C. Puhl, Kimberley M. Zorn, Thomas R. Lane, Daniel P. Russo, Jennifer J. Klein, Anthony J. Hickey, and Alex M. Clark. Exploiting machine learning for end-to-end drug discovery and development. *Nature Materials* **18**, 435-441 (2019).
- 32 Stokes, J. M. e. a. A deep learning approach to antibiotic discovery. *Cell* **180** (2020).
- 33 Paula Carracedo-Reboredo, J. L.-B., Nereida Rodríguez-Fernández, Francisco Cedrón, Francisco J. Novoa, Adrian Carballal, Victor Maojo, Alejandro Pazos, Carlos Fernandez-Lozano. A review on machine learning approaches and trends in drug discovery. *Computational and Structural Biotechnology Journal* **19**, 4538-4558, doi:10.1016/j.csbj.2021.08.011 (2021).

- 34 Schütt, K. T., Arbabzadah, F., Chmiela, S., Müller, K. R. & Tkatchenko, A. Quantum-chemical insights from deep tensor neural networks. *Nat. Commun. Nat. Commun.* **8** (2017).
- 35 Unke, O. T., and Markus Meuwly. PhysNet: A neural network for predicting energies, forces, dipole moments, and partial charges. *Journal of chemical theory and computation* **15**, 3678-3693.
- 36 Viraj Bagal, R. A., P. K. Vinod, and U. Deva Priyakumar*. MolGPT: Molecular Generation Using a Transformer-Decoder Model. *J. Chem. Inf. Model* **62**, 2064-2076 (2022).
- 37 Zhenqin Wu, B. R., Evan N. Feinberg, Joseph Gomes, Caleb Geniesse, Aneesh S. Pappu, Karl Leswing and Vijay Pande. MoleculeNet: a benchmark for molecular machine learning. *Chem. Sci.* **9**, 513-530 (2018).
- 38 Zubatyuk, R., Smith, J. S., Leszczynski, J. & Isayev, O. Accurate and transferable multitask prediction of chemical properties with an atoms-in-molecules neural network. *Sci. Adv.* **5** (2019).
- 39 Chen, C., Weiye Ye, Yunxing Zuo, Chen Zheng, and Shyue Ping Ong. Chen, Chi, et al. "Graph networks as a universal machine learning framework for molecules and crystals. *Chemistry of Materials* **31**, 3564-3572 (2019).
- 40 Choudhary, K., and Brian DeCost. Atomistic Line Graph Neural Network for improved materials property predictions. *npj Computational Materials* **7**, 1-8 (2021).
- 41 Shui, Z., & Karypis, G. in *2020 IEEE International Conference on Data Mining (ICDM)* 492-500 (2020).
- 42 Zhang, S., Yang Liu, and Lei Xie. . Molecular mechanics-driven graph neural network with multiplex graph for molecular structures. *arXiv preprint* (2020).
- 43 EJ Bjerrum, R. T. Molecular generation with recurrent neural networks (RNNs). *arXiv preprint arXiv:1705.04612*, doi:arXiv:1705.04612 (2017).
- 44 Olivecrona, M., Thomas Blaschke, Ola Engkvist, and Hongming Chen. Molecular de-novo design through deep reinforcement learning. *Journal of Cheminformatics* **9**, 1-14 (2017).
- 45 Popova, M., Olexandr Isayev, and Alexander Tropsha. Deep reinforcement learning for de novo drug design. *Science Advances* **4** (2018).
- 46 Schütt, K., Pieter-Jan Kindermans, Huziel Enoc Sauceda Felix, Stefan Chmiela, Alexandre Tkatchenko, and Klaus-Robert Müller. Schnet: A continuous-filter convolutional neural network for modeling quantum interactions. *Advances in Neural Information Processing Systems* **30** (2017).
- 47 Thomas Blaschke, M. O., Dr. Ola Engkvist, Prof. Jürgen Bajorath, Dr. Hongming Chen. Application of Generative Autoencoder in De Novo Molecular Design. *Molecular Informatics* **37**, 1700123 (2018).
- 48 Camille Bilodeau, W. J., Tommi Jaakkola, Regina Barzilay, Klavs F. Jensen. Generative models for molecular discovery: Recent advances and challenges. *Computational Molecular Science* **5**, e1608 (2022).
- 49 Anvita Gupta, A. T. M., Berend J. H. Huisman, Jens A. Fuchs, Petra Schneider, Gisbert Schneider. Generative Recurrent Networks for De Novo Drug Design. *Molecular Informatics* **37**, 1700111 (2017).
- 50 Martinelli, D. D. Generative machine learning for de novo drug discovery: A systematic review. *Computers in Biology and Medicine* **145**, 105403 (2022).

- 51 Zhaoping Xiong, D. W., Xiaohong Liu, Feisheng Zhong, Xiaozhe Wan, Xutong Li, Zhaojun Li, Xiaomin Luo, Kaixian Chen, Hualiang Jiang*, and Mingyue Zheng. Pushing the Boundaries of Molecular Representation for Drug Discovery with the Graph Attention Mechanism. *J. Med. Chem.* **63**, 8749-8760 (2019).
- 52 Xian-bin Ye, Q. G., Weiqi Luo, Liangda Fang, Zhao-Rong Lai, Jun Wang. Molecular substructure graph attention network for molecular property identification in drug discovery. *Pattern Recognition* **128**, 108659 (2022).
- 53 Huihui Yan, Y. X., Yao Liu, Leer Yuan, Rong Sheng. ComABAN: refining molecular representation with the graph attention mechanism to accelerate drug discovery. *Briefings in Bioinformatics* **23**, bbac350 (2022).
- 54 Grisoni, D. v. T. a. F. Traversing Chemical Space with Active Deep Learning in Low-data Scenarios. *Chemrxiv*, doi:10.26434/chemrxiv-2023-wgl32-v2 (2023).
- 55 Sergei V Kalinin, M. P. O., Mani Valletti, Junjie Zhang, Raphael P Hermann, Hong Zheng, Wenrui Zhang, Gyula Eres, Rama K Vasudevan, Maxim Ziatdinov. Deep Bayesian local crystallography. *npj Computational Materials* **7**, 181 (2021).
- 56 Sergei V Kalinin, S. Z., Mani Valletti, Harley Pyles, David Baker, James J De Yoreo, Maxim Ziatdinov. Disentangling Rotational Dynamics and Ordering Transitions in a System of Self-Organizing Protein Nanorods via Rotationally Invariant Latent Representations. *ACS Nano* **15**, 6471-6480 (2021).
- 57 Ayana Ghosh, S. V. K., Maxim A Ziatdinov. Discovery of structure-property relations for molecules via hypothesis-driven active learning over the chemical space. *APL Mach. Learn.* **1**, 046102 (2023).
- 58 Gagliardi*, O. R. a. A. Deep Learning Total Energies and Orbital Energies of Large Organic Molecules Using Hybridization of Molecular Fingerprints. *Journal of Chemical Information and Modeling* **60**, 5971-5983 (2020).
- 59 Gómez-Bombarelli, R. W., J.N.; Duvenaud, D.; Hernández- Lobato, J. M.; Sañchez-Lengeling, B.; Sheberla, D.; Aguilera- Iparraguirre, J.; Hirzel, T. D.; Adams, R. P.; Aspuru-Guzik, A. Automatic Chemical Design Using a Data-Driven Continuous Representation of Molecules. *ACS Cent. Sci.* **4**, 268-276 (2018).
- 60 Zachary Fox, A. G. in *AI for Accelerated Materials Design-NeurIPS 2023 Workshop* (2023).
- 61 Mani Valletti, R. K. V., Maxim A Ziatdinov, Sergei V Kalinin. Bayesian optimization in continuous spaces via virtual process embeddings. *Digital Discovery* **1**, 15 (2022).
- 62 Komodakis, M. S. N. in *Artificial Neural Networks and Machine Learning - ICANN 2018*. (Springer).
- 63 Rafael Gómez-Bombarelli, J. N. W., ## David Duvenaud, ¶ José Miguel Hernández-Lobato, § Benjamín Sánchez-Lengeling, ‡ Dennis Sheberla, ‡ Jorge Aguilera- Iparraguirre, † Timothy D. Hirzel, † Ryan P. Adams, ∇ and Alán Aspuru-Guzik corresponding author* ‡ ⊥. Automatic Chemical Design Using a Data-Driven Continuous Representation of Molecules. *ACS Cent. Sci.* **4**, 268-276 (2018).
- 64 Yongtao Liu, M. Z., Sergei V Kalinin. Exploring causal physical mechanisms via non-gaussian linear models and deep kernel learning: applications for ferroelectric domain structures. *ACS nano* **16**, 1250-1259 (2021).

- 65 Maxim Ziatdinov, Y. L., Sergei V Kalinin. Active learning in open experimental environments: selecting the right information channel (s) based on predictability in deep kernel learning. *arXiv preprint arXiv:2203.10181*, doi:arXiv:2203.10181 (2022).
- 66 Maxim Ziatdinov, A. G., Sergei V Kalinin. Physics makes the difference: Bayesian optimization and active learning via augmented Gaussian process. *Machine Learning: Science and Technology* **3**, 015022, doi:10.1088/2632-2153/ac4baa (2021).
- 67 Maxim Ziatdinov, Y. L., Kyle Kelley, Rama Vasudevan, Sergei V Kalinin. Bayesian active learning for scanning probe microscopy: from gaussian processes to hypothesis learning. *ACS nano* **16**, 13492-12512 (2022).
- 68 Maxim A Ziatdinov, Y. L., Anna N Morozovska, Eugene A Eliseev, Xiaohang Zhang, Ichiro Takeuchi, Sergei V Kalinin. Hypothesis learning in automated experiment: application to combinatorial materials libraries. *Advanced Materials*, 22013345 (2022).
- 69 Kanagawa, M. a. H., P. and Sejdinovic, D. and Sriperumbudur, B. K. Gaussian Processes and Kernel Methods: A Review on Connections and Equivalences. *arXiv preprint arXiv:1805.08845v1* (2018).
- 70 Ping Li, S. C. A review on Gaussian Process Latent Variable Models. *CAAI Transactions on Intelligence Technology* **1** (2016).
- 71 Shahriari B, S. K., Wang Z, Adams R P and Freitas N D. Taking the human out of the loop: A review of Bayesian optimization. *Proc. IEEE* **104**, 148-175 (2016).
- 72 J, K. H. A versatile stochastic model of a function of unknown and time varying form. *Math. Anal. Appl.* **5**, 150-167 (1962).
- 73 J, K. H. A new method of locating the maximum point of an arbitrary multipeak curve in the presence of noise. *J. Basic Eng.* **86**, 97-106 (1964).
- 74 Wilson, A. G. & Nickisch, H. in *Proceedings of the 32nd International Conference on International Conference on Machine Learning - Volume 37* 1775–1784 (JMLR.org, Lille, France, 2015).
- 75 Wilson, A. G., Hu, Z., Salakhutdinov, R. & Xing, E. P. in *Artificial intelligence and statistics*. 370-378 (PMLR).
- 76 Wilson, A. & Adams, R. in *International conference on machine learning*. 1067-1075 (PMLR).
- 77 Grégoire Ferré, T. H., and Kipton Barros. Learning molecular energies using localized graph kernels. *Journal of Chemical Physics* **146** (2017).
- 78 Ramakrishnan, R., and O. Anatole von Lilienfeld. Many molecular properties from one kernel in chemical space. *CHIMIA International Journal for Chemistry* **69**, 182-186 (2015).
- 79 Johannes A. Mohr, B. J. J., and Klaus Obermayer†. Molecule Kernels: A Descriptor- and Alignment-Free Quantitative Structure–Activity Relationship Approach. *Journal of Chemical Information and Modeling* **48**, 1868-1881 (2008).
- 80 Hiroshi Yamashita, T. H., and Ryo Yoshida. Atom Environment Kernels on Molecules. *Journal of Chemical Information and Modeling* **54**, 1289-1300 (2014).
- 81 AG Wilson, Z. H., R Salakhutdinov, EP Xing. in *19th International Conference on Artificial Intelligence and Statistics*. (Journal of Machine Learning Research).
- 82 CE Rasmussen, C. W. *Gaussian processes for machine learning*. Vol. 1 (MIT press, 2006).
- 83 Ramakrishnan, R., Dral, P., Rupp, M. & vonLilienfeld, O. A. Quantum chemistry structures and properties of 134 kilo molecules. *Sci. Data* **1**, 140022 (2014).

